Integrated sensing and acoustofluidic functions for flexible thin film acoustic wave devices based on metallic and polymer multilayers

Shahrzad Zahertar, Ran Tao, Hongzhe Wang, Hamdi Torun, Pep Canyelles-Pericas, Yang Liu, Jethro Vernon, Wai Pang Ng, Richard Binns, Qiang Wu, Jingting Luo, Yong-Qing Fu

***Abstract*— Surface acoustic wave (SAW) devices are generally fabricated on rigid substrates that support the propagation of waves efficiently. Although very challenging, the realisation of SAW devices on bendable and flexible substrates can lead to new generation SAW devices for wearable technologies. In this paper, we report flexible acoustic wave devices based on ZnO thin films coated on various substrates consisting of thin layers of metal (e.g., Ni/Cu/Ni) and/or polymer (e.g., polyethylene terephthalate, PET). We comparatively characterise the fabricated SAW devices and demonstrate their sensing applications for temperature and ultraviolet (UV) light. We also investigate their acoustofluidic capabilities on different substrates. Our results show that the SAW devices fabricated on a polymer layer (e.g. ZnO/PET, ZnO/Ni/Cu/Ni/PET) show enhanced temperature responsivity, and the devices with larger wavelengths are more sensitive to UV exposure. For actuation purposes, the devices fabricated on ZnO/Ni/Cu/Ni layer have the best performance for acoustofluidics, whereas insignificant acoustofluidic effects are observed with the devices fabricated on ZnO/PET layers. We propose that the addition of a metallic layer of Ni/Cu/Ni between ZnO and polymer layers facilitates the actuation capability for the acoustofluidic applications while keeping temperature and UV sensing capabilities, thus enhancing the integration of sensing and acoustofluidic functions.**

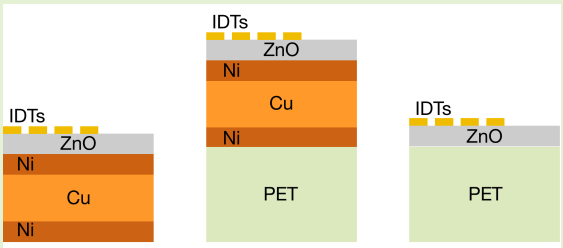

***Index Terms*— Acoustic wave, thin film, flexible, bendable, sensing, acoustofluidics, multilayers**

This work was supported by the Engineering Physics and Science Research Council of UK (EPSRC EP/P018998/1) and UK Fluidic Network (EP/N032861/1) -Special Interest Group of Acoustofluidics, Network Plus in Digitalised Surface Manufacturing (EP/S036180/1), Royal Society International Exchange grant with NSFC Newton Mobility Grant (IEC/NSFC/201078), as well as National Science Foundation of China (No. 61774028 and 92064004).

Corresponding Author: Prof. Richard Y.Q. Fu (e-mail: richard.fu@northumbria.ac.uk)

S. Zahertar, R. Tao, H. Wang, P. Canyelles-Pericas, J. Luo were with Faculty of Engineering & Environment, University of Northumbria, Newcastle upon Tyne, NE1 8ST, UK.

S. Zahertar (e-mail: s.zahertar@soton.co.uk) is now affiliated with the Optoelectronics Research Centre, University of Southampton, Southampton, SO17 1BJ, UK.

R. Tao (e-mail: ran.tao@szu.edu.cn) and J. Luo (email: luojt@szu.edu.cn) are now affiliated with Shenzhen Key Laboratory of Advanced Thin Films and Applications, College of Physics and Optoelectronic Engineering, Shenzhen University 518060, China.

H. Wang (email:wanghongzhe93@gmail.com) and Y. Liu (email:yliu1975@uestc.edu.cn) are now with State Key Laboratory of Electronic Thin Films and Integrated Devices, University of Electronic Science and Technology of China, Chengdu, 610054, P. R. China.

H. Torun (e-mail: hamdi.torun@northumbria.ac.uk), J. Vernon (e-mail: jethro.vernon@northumbria.ac.uk), W. P. Ng (e-mail: wai-pang.ng@northumbria.ac.uk), R. Binns (e-mail: richard.binns@northumbria.ac.uk), Q. Wu (e-mail: qiang.wu@northumbria.ac.uk), and Y.Q. Fu (e-mail: richard.fu@northumbria.ac.uk) are with Faculty of Engineering & Environment, University of Northumbria, Newcastle upon Tyne, NE1 8ST, UK.

P. Canyelles-Pericas is now affiliated with Department of Integrated Devices and Systems, MESA+ Institute, University of Twente, Enschede, 7522 NB, the Netherlands (e-mail: j.canyellespericas@utwente.nl).

I. Introduction

RAPID developments in the fields of biosensing and microfluidics pave the way for the delivery of effective lab-on-chip (LOC) devices. LOC, as its name suggests, aims to bring the whole laboratory processes onto a small chip, and therefore is presented as an integrated platform capable of performing different functions such as liquid preparation, sampling and sensing [1], [2]. Despite the technological advancements in these fields, there are remaining challenges, for instance, integrating two main components that are needed for delivery of a market-ready LOC product, e.g., sensing and actuating. Sensors can detect various chemical, biological, or physical entities, and they are applied in many fields such as product quality control and assessment, air quality measurements, healthcare, food industry and security. Actuators are needed in LOC to manipulate liquid or droplets for sample preparation, treatment, and removal. Combining sensors and actuators in a single device would reduce the manufacturing complexity of the LOC and thus its cost. This would be very convenient for healthcare wearable devices, which are typically employed for single uses. In particular, there has also been much attention paid to flexible and wearable devices in recent years for applications such as personalised or portable healthcare devices [3]–[5], e-skin and human-robot

interactions [6]–[10], and chemical sensing [11]–[16].

Surface acoustic wave (SAW) sensors and actuators can generate and detect acoustic waves confined dominantly near the surface layer using interdigitated transducers (IDTs) on a piezoelectric layer [17]–[19], and have been investigated for microfluidics applications [20]–[22]. Different functions such as streaming, pumping, jetting, and atomization can be achieved by controlling the frequency and power applied to the IDT electrodes for a targeted liquid with different material properties [23]. This feature can be especially advantageous for non-invasive, rapid and reliable disease diagnosis applications, minimal liquid consumption, reduced sample analysis time and therefore reduced cost [22], [24]. Also, SAWs have been employed for sensing various environmental parameters such as the temperature and the UV light [25]–[28]. Therefore, having both capabilities of sensing and fluid actuation, these devices are attractive to be integrated into LOC platforms.

Flexible SAW devices with multiple functionalities can be realised using thin-film acoustic wave actuators, such as those based on zinc oxide (ZnO) on conformable substrates of aluminium foil [26], [29], [30] and/or different types of polymers [31]–[34] . They have been used for sensing and microfluidics with similar performance to their rigid counterparts. However, there are still challenges for thin film flexible acoustic wave devices on either metal substrates (deformability/wrinkling of thin metallic layers after multiple use) or polymer (significant wave damping and reduced efficiency for acoustofluidics) [33], [34].

In this work, we report three types of flexible and bendable SAW devices that are suitable for different sensing and actuation purposes, which can be effectively integrated into a lab-on-chip. The devices are composed of a ZnO thin film (as the piezoelectric layer for acoustic wave generation) deposited on a layer of metallic or polymer thin films, or both. We propose a solution to improve the acoustofluidic capability of SAW devices on polymers by adding metallic films between the piezoelectric and the polymer layers. The metallic thin films are consisted of trilayers of nickel, copper, and nickel (e.g., Ni/Cu/Ni). Ni is resistant to wear and corrosion and plating metals with Ni can improve their durability and resistance to corrosion of Cu [35]–[37]. The utilised polymer layer in this study is polyethylene terephthalate (PET). We characterise the fabricated devices, demonstrate their sensing capability for temperature and UV light, and comparatively investigate their acoustofluidic performances for fluid manipulation. This work is the extended version of the paper presented at the 2021 IEEE International Conference on Flexible and Printable Sensors and Systems (FLEPS) and some of the data was published in its Proceedings [38].

II. Methodology

A. Device Fabrication

Three different types of devices were fabricated in this study. ZnO film with a thickness of $\sim$ 5 μm was selected as the piezoelectric layer for all the devices (the cross-section schematic of the fabricated devices is shown in Supplementary Fig. S1). The fabricated devices are composed of multi-layers of: (a) ZnO/Ni/Cu/Ni (b) ZnO/Ni/Cu/Ni/PET and (c) ZnO/PET. Ni/Cu/Ni films with their thicknesses of 1, 23, 1 μm for each layer, respectively, were obtained from Shenzen Vanlead Technology Co. LTD., China. The commercial PET substrate has a thickness of 125 μm and was bonded to Ni/Cu/Ni substrates through a roll-to-roll process. For the ease of recalling the fabricated devices within the text, the Ni/Cu/Ni trilayers will be named as the "*Trimetal*" layer throughout the text.

ZnO film was deposited on the substrates using a direct current (DC) magnetron sputter. DC power of 400 W was used for the zinc target with a purity of 99.99%, with Ar/O_2 gas flow rate of 6/13 sccm, and a pressure level of 6×10^{-4} mbar. The film thickness was controlled to be $\sim$ 5 μm and uniformity was achieved by rotating the sample holders during the deposition process. Interdigital transducers (IDTs) were patterned on the substrates utilising standard photolithography and lift-off processes. For the photolithography, S1813 ([39]) was used as the photoresist and was spin coated on the ZnO coated substrates. Then the substrates were softly baked at 110 °C for five minutes. A mask aligner (EVG620) was utilised for exposing the substrates to UV light with an intensity of 75 mJ/cm^2 for the duration of 7 seconds and the developing time was $\sim$ 1 minute. Cr/Au layers with thicknesses of 20/100 nm were deposited on the substrates using a thermal evaporator (EDWARDS AUTO306) and the patterns of the electrodes were obtained using a standard lift-off process. The IDTs were fabricated with wavelengths, λ, of 64, 100 and 160 μm.

B. Experimental Methods

For device characterisation, the reflection spectra of the fabricated devices were obtained using a vector network analyser (Keysight N9913A). To measure the temperature coefficient of frequency (TCF) of the devices, the temperature was varied from room temperature up to around 100 °C in an oven and verified with a temperature sensor that was attached on top of the acoustic wave devices. To evaluate the responses of the fabricated devices with various IDT wavelengths on ZnO/Trimetal/PET to the ultraviolet (UV) light, the devices were connected to the vector network analyser and placed under a UV gun (CS2010; Thorlabs Inc., Newton, NJ). UV intensity of 151.20 mW/cm^2 for the duration of 22 seconds was applied to perform the experiments. The wavelength of the UV light was 365 nm. A LabVIEW (National Instruments Inc.) based program was developed to implement real-time measurements of frequency changes of the flexible SAW UV sensors. To observe the effect of viscosity of a droplet on the resonant frequency of the device, various volumetric solutions of glycerol and DI water with the following ratios were prepared; 3:1, 1:1, and 1:3 (DI water/glycerol). Subsequently, a droplet of 10 μl of each solution from the lowest viscosity to the highest viscosity was placed on the IDTs of the SAW device sequentially and the resonant frequency was measured using the VNA. The surface of the SAW device was cleaned before applying a new droplet.

For performing acoustofluidic experiments, the surfaces of the fabricated devices were treated with a hydrophobic layer of 1% CYTOP solution (L-809A) by dip-coating and were heated

to 150 °C for ∼5 minutes. The SAW devices were connected to an RF signal generator (Marconi Instruments, 9 kHz-2.4 GHz 2024) through a power amplifier (Amplifier Research, model 75A250) and were acoustically excited. A droplet of 1 μl of deionised water was placed in front of the IDTs, and the droplet movement was captured using a conventional video camera.

C. Simulation

Finite Element Analysis (FEA) was performed for SAW device using a commercial package (COMSOL Multiphysics) with solid mechanics, electrostatics, and pressure acoustic modules. A 2D layered model utilising a pair of IDTs with periodic boundary conditions were applied in simulations. The model included layers of Ni, Cu, Ni, and the piezoelectric layer of ZnO from bottom to top. These layers were designed with thicknesses of 1 μm, 23 μm, 1 μm, and 5 μm, respectively. An IDT comprising finger electrodes made of gold with the thickness of 120 nm, width of 25 μm, and length of 300 μm was built on top of the piezoelectric layer. Vibration patterns and frequency modes were obtained by eigenfrequency calculations using the COMSOL Multiphysics software.

III. Results and Discussion

A. Characterisation of SAW Devices

The simulation and experimental reflection S_{11} spectra of the fabricated ZnO/TrimetalNi/Cu/Ni devices with different wavelengths of 64, 100 and 160 μm were obtained using COMSOL Multiphysics and a vector network analyser, respectively. The results are shown in Fig. 1. The acoustic resonant frequency (f) is determined by the phase velocity of acoustic wave (ν) in the substrate and the wavelength (λ) of the IDTs ($f = \nu/\lambda$). As expected, by increasing the wavelength of IDTs, the acoustic frequencies of the devices shift towards lower values. Lamb waves are usually generated in thin structures, where the thickness of the substrate is smaller than the designed wavelength. Two types of Lamb waves can be present in thin membranes at lower frequencies; 1) flexural or anti-symmetric (A-mode), 2) extensional or symmetric (S-mode) [40]–[43]. The modes of acoustic frequencies are labelled in the experimental results as shown in Fig. 1. The first resonant frequency is asymmetric lamb wave (A_0) mode, the second frequency is symmetric lamb wave (S_0) mode, while the third or further frequency (if any) in the S_{11} spectrum corresponds to higher order modes of Lamb waves.

We have confirmed the wave modes with the help of simulations. Fig. 1(a) shows a comparison between the simulation and experimental data for the device with an IDT wavelength of 100 μm as an example together with frequency modes as insets. The experimentally measured resonant frequencies for A_0 and S_0 modes are in good agreements with the simulations and the discrepancies between simulation and experimental results can be due to several factors. For example, the selection of specific numerical simulation parameters such as mesh and sweep settings can affect the results. Also, the material properties used in simulation can be slightly different than the actual values of the samples. Another reason could be the fabrication-related issues, such as IDT metal deposition and patterning and imperfection in the ZnO layer, or the Trimetal layer.

The obtained experimental results for devices on ZnO/Trimetal substrate for all the designed wavelengths are illustrated in Fig. 1(b), while Fig. 1(c) and Fig. 1(d) represent the reflection spectra of devices fabricated on ZnO/Trimetal/PET and ZnO/PET substrates, respectively.

Although the total substrate thickness is increased when a PET layer is added to the Trimetal layers, the acoustic frequencies are remained unaltered, inferring that the created mode is evanescent and that the wave is bounded at the surface of the added PET layer. This can be seen from the experimental results shown in Fig 1(b) and Fig1 (c). Mechanical interactions between the SAW and subsequent layers influence the SAW propagation velocity and power dissipation and attenuation of the waves [44]. As anticipated, the PET layer leads to significant attenuation of acoustic wave energy into the substrate and therefore, the resonant peaks are weaker compared to other substrates. This can be clearly observed in Fig. 1(c) and Fig. 1(d). Although both of the devices contain the same PET layer, the device including the 25 μm of Trimetal layer effectively enhances the acoustic performance. In other words, the substrates that include Trimetal layers can be acoustically excited more efficiently at lower frequencies compared to ZnO/PET devices.

B. SAW Sensing Functions

One of the advantages of SAW actuators is that they can be used for various sensing applications. The resonant frequency of SAW devices can be influenced and altered by several factors including mass loading, conductivity, temperature, etc. Monitoring the changes in the resonant frequency caused by these factors can be utilised as a sensing mechanism following the equation (1) [45]:

$$\begin{aligned}\frac{\Delta f}{f_0} &= \frac{\Delta \nu}{\nu} \\ &= \frac{1}{\nu}\Big(\frac{\partial \nu}{\partial m}\Delta m + \frac{\partial \nu}{\partial \sigma}\Delta\sigma + \frac{\partial \nu}{\partial T}\Delta T + \frac{\partial \nu}{\partial c}\Delta c + \\ &\quad \frac{\partial \nu}{\partial \varepsilon}\Delta\varepsilon + \frac{\partial \nu}{\partial P}\Delta P + \frac{\partial \nu}{\partial \eta}\Delta\eta + \frac{\partial \nu}{\partial \rho}\Delta\rho + \ldots\Big) \quad (1)\end{aligned}$$

where m is the mass load, σ is the conductivity, T is the temperature, c is the mechanical constant, ε is the dielectric constant, P is the pressure, η is the viscosity, and ρ is the density. TCF is theoretically defined by the following equation (2) [45]:

$$TCF = \frac{1}{f_0}\frac{\partial f}{\partial T} = \frac{1}{\nu_p}\frac{\partial \nu_p}{\partial T} - \frac{1}{\lambda}\frac{\partial \lambda}{\partial T} = \frac{1}{\nu_p}\frac{\partial \nu_p}{\partial T} - \alpha \quad (2)$$

where f_0, T are the reference frequency and temperature; and ν_p, λ, and α are phase velocity, wavelength, and thermal expansion coefficient of the device, respectively. With the PET as the substrate for the SAW device it can cause significant temperature effect on the device. The TCF value depends on the defined elements, and by using a PET layer as the SAW

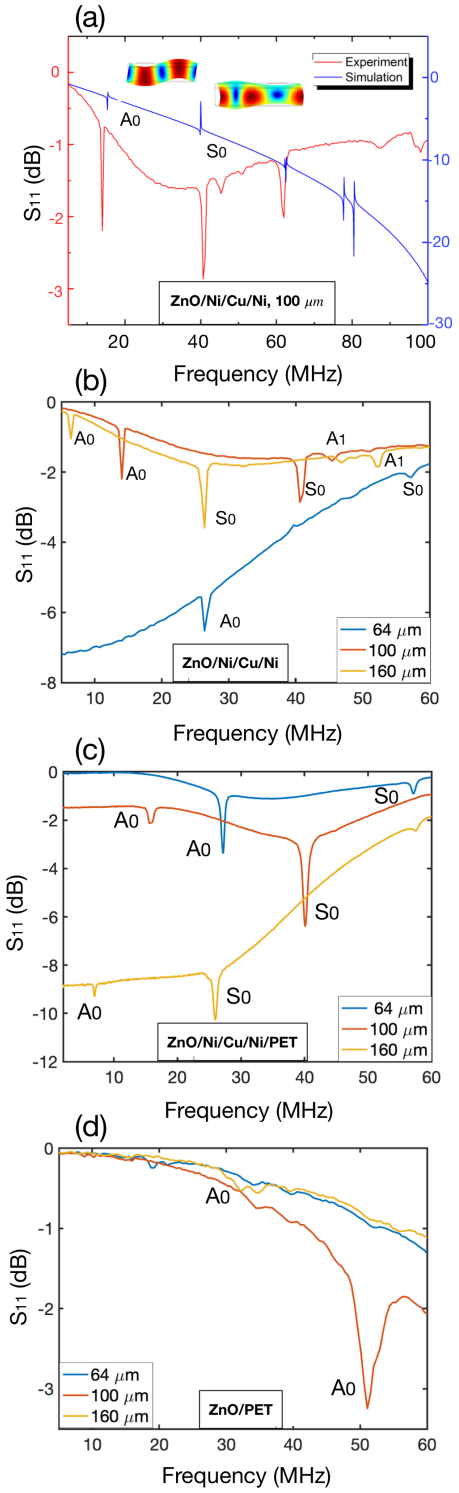

Fig. 1. (a) Comparisons between simulation and experimental results of resonant frequencies for the designed wavelength of 100 μm for ZnO/Trimetal substrate, experimentally obtained reflection spectra for various wavelengths for (b) ZnO/Trimetal substrate, (c) ZnO/Trimetal/PET substrate and (d)ZnO/PET substrate.

substrate, thermal expansion coefficient is altered dramatically, which leads to higher absolute values of TCF.

Fig. 2(a) depicts the absolute TCF values of all three types of SAW devices. As is shown in the obtained data, the TCF

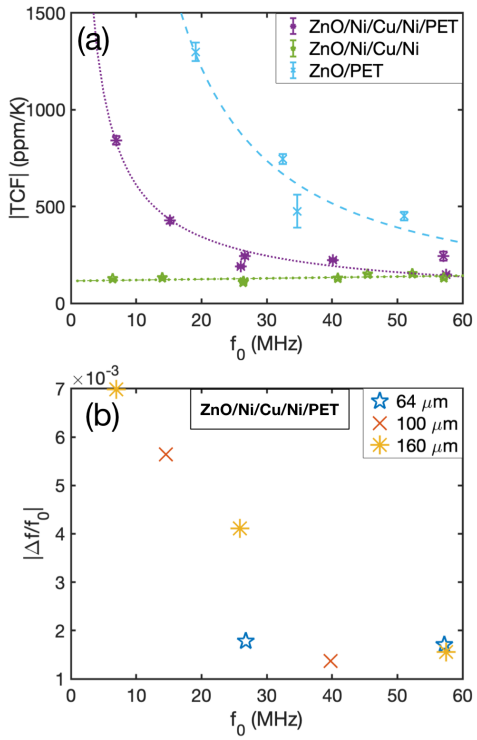

Fig. 2. (a) Absolute TCF values for the three fabricated substrates; (b) UV Sensing of ZnO/Trimetal/PET substrate.

value remains almost constant for ZnO/Trimetal substrate, whilst it changes significantly with temperature for the devices that include a PET layer. For the substrate of the PET layer, the absolute value of TCF can reach very large levels of 1295 and 822 ppm/K for ZnO/PET and ZnO/Trimetal/PET SAW devices, respectively, and the TCF value decreases with the increase of frequency in those devices. It can be seen from Fig. 2 that ZnO/PET device has the highest TCF value among these three devices, however, the SAW actuation is significantly weaker in this type of device compared to previous ones as will be explained in the next section. This can be due to the significant loss of acoustic energy in the polymer layer as energy would also be significantly dissipated into the soft polymer.

Devices fabricated on ZnO/Trimetal/PET layers showed a strong temperature-induced responsivity with distinct frequency peaks in acoustic characterisation. Therefore, we selected this type of substrate to investigate its response to high intensity UV exposures and explore the effects of IDT wavelengths. Based on the equation 1, the frequency change due to UV exposure can be attributed to two main factors, e.g., (a) the conductivity change in ZnO, and (b) the temperature change caused by the UV exposure. The frequency shift based on the conductivity change can be described utilising the equation (3) [46]:

$$\frac{\Delta f}{f_0} = \frac{\Delta \nu}{\nu_0} = -\frac{k^2}{2}\frac{1}{1+(\nu_0 C_s/\sigma_s)^2} \tag{3}$$

where k^2 is the coupling coefficient, C_s is the capacitance per unit length of the surface, and σ_s is the sheet conductivity.

Recently we reported that increasing the UV intensity also increases the sheet conductivity in the ZnO thin film and that the frequency shift caused by UV-induced temperature change can be negligible compared to the total frequency shift in high intensities of UV exposure [47]. In this study, we selected a fixed intensity of UV exposure, and we investigated the effects of various wavelengths to the response of the fabricated devices to the UV exposure. Fig. 2(b) depicts normalised frequency differences versus reference frequency for UV intensity of 151.20 mW/cm^2 and the duration of 22 s. As shown in this figure, asymmetric lamb wave mode (A_0) is more responsive to the UV light and the value of normalised frequency difference is higher in this mode of frequency compared to the rest. Also, devices with higher designed wavelengths show a more significant change compared to smaller wavelengths. Therefore, devices with higher designed wavelengths calibrated at their lower frequency modes might be more desirable for the applications where the UV intensity needs to be carefully monitored. Further investigations on other various possible wavelengths and substrates in the future would help obtain an empirical equation to explain this effect and generalise the conclusion.

In the next set of sensing experiments, we selected ZnO/Trimetal/PET substrate with the wavelength of 100 μm and measured the responses of the device to various viscosities. For this purpose, we prepared various glycerol volumetric solutions, with glycerol to DI proportions of 0% (DI), 25%, 50%, and 75%. We placed 10 μl droplet of each solution on top of the IDTs and recorded the S_{11} spectra, respectively. The results are plotted in Fig. 3. The nominal frequency of the device is ~17.93 MHz and addition of the droplet on the IDTs results in a shift in nominal frequency towards lower values. The corresponding nominal frequencies with the presence of the droplet are 17.87, 17,86, 17.85, and 17.83 MHz for DI, 25%, 50%, and 75% of glycerol respectively. The changes we observe in the acoustic frequency by loading droplets could be a combination of mass-loading, dielectric loading and viscosity changes. By placing a water droplet, compared to the case where there is no droplet present on the IDTs, the frequency shift would be mostly dominated by the mass or dielectric loading. However, since the density is changed from 1 to 1.19 g/cm^3 (e.g., from water to 75% Glycerol, respectively), the mass difference would be negligible. Therefore, further change in the acoustic frequency would be mostly attributed to the viscosity change According to equation (1), mass-loading and increased viscosity lead to a larger shift in the frequency, which is in agreement with the experimental results depicted in Fig. 3(a). Sample S_{11} spectra in a narrowed frequency range for these solutions are presented in Fig. 3(b).

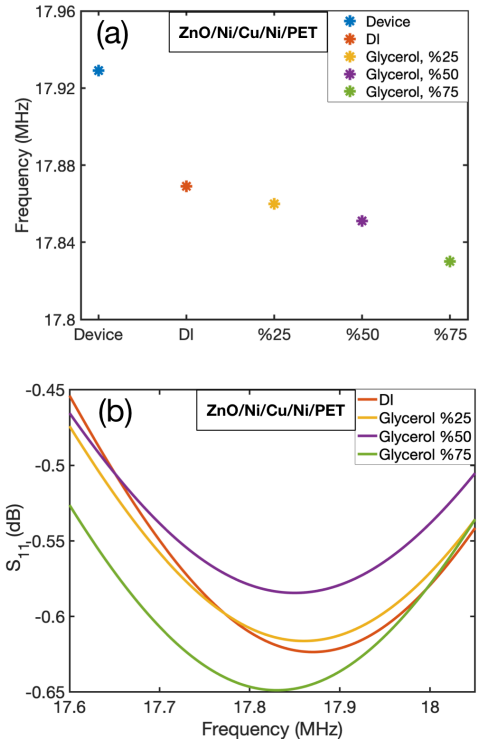

Fig. 3. (a) Frequency values for different viscosities; (b) Sample S_{11} plots for various Glycerol volumetric solutions in DI.

C. Acoustofluidic Performance

In the next set of experiments, the microfluidic actuation capability of the fabricated devices was tested.

Fig. 4(a) illustrates the pumping speeds of the droplet for the device with the wavelength of 100 μm fabricated on ZnO/Trimetal layers versus different powers at an operating frequency of 14 MHz. For this experiment, a droplet of 1 μl was placed in front of IDTs. The droplet started to move with the applied power of 3.8 W and by further increasing the applied power, the droplet was pumped at higher speeds up to 9.55 mm/s with a power of 7 W and then decreased to 5.2 mm/s by applying a power of 7.8 W. The decrease in speed after 7 W could be due to the heating effect, which means that at higher powers, not all the energy is transferred to the droplet and part of energy is converted to heat and might be dissipated into the film. In addition to the loss of energy transferred to the droplet, the resonant frequency of the device is altered due to heating that also degrades the pumping performance. During the pumping process, deformation of the ZnO/Trimetal SAW device can be observed, and device has bent upwards due to the bimetallic effect caused by the SAW induced heating.

We also investigated the pumping capability of the devices fabricated on ZnO/PET layers. However, due to the excessive acoustic energy loss into the polymer layer, we did not observe any significant acoustofluidic functions (except significant internal streaming effect) on these substrates. In order to solve this issue, the pumping capability of devices fabricated on ZnO/Trimetal/PET layers was explored. Fig. 4(b) depicts the obtained results for the applied power at 8.2 MHz, where a droplet of 1 μl was placed in front of the IDTs with the wavelength of 160 μm. In this case, pumping occurred from 1.6 W up to 4.5 W. The pumping speed started from 0.008 mm/s for the power of 1.8 W and reached its maximum of 0.52 mm/s at the applied power of 3.6 W. After this point, further increasing RF power led to lower speed for pumping, which could be a result of significant heat generation at such higher powers.

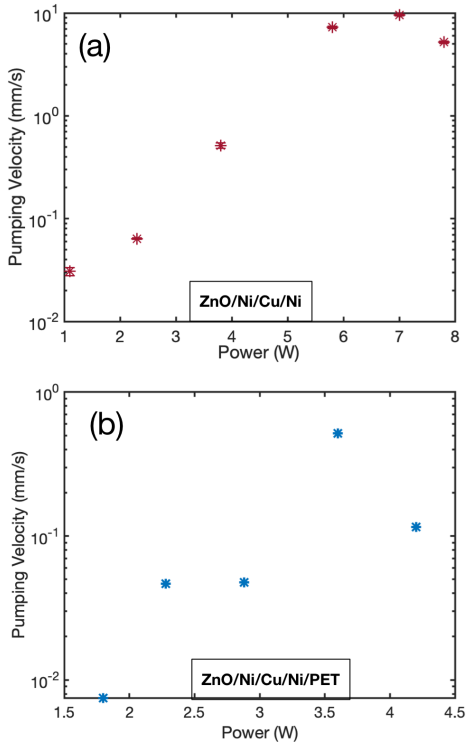

Fig. 4. (a) Pumping velocity of ZnO/Trimetal; (b) Pumping velocity of ZnO/Trimetal/PET.

The lack of acoustofluidic activity in ZnO/PET substrates could be attributed to the following reasons. In the devices composing Trimetal layers and by considering the 5 μm thickness of the ZnO film, deposition of IDTs on top of the substrates would create vertical electric fields under IDTs, which are stronger than the lateral fields along the $\lambda/4$ gaps (16 μm and higher) between the opposite polarity IDT fingers. The vertical fields also couple to the predominant piezoelectric constant of ZnO. As a result, energy trapping in the relatively thick Trimetal layers concentrates the acoustic energy in the lower loss materials, avoiding crystal grain boundary losses in ZnO and polymer losses in PET. By comparing the results among these three substrates, we can see clearly that by adding a metallic layer between the piezoelectric and polymer layers has prevented the excessive loss of acoustic energy and has significantly improved the acoustofluidic capability of the device.

IV. Conclusion

We have introduced three types of flexible and bendable SAW devices utilising ZnO thin film as the piezoelectric layer deposited on thin metallic (Ni/Cu/Ni, Trimetal), polymer (PET) layers and combined Ni/Cu/Ni and PET. We investigated the TCF responses of the fabricated SAW devices to the temperature changes. We observed that devices which included PET layer in their substrate showed stronger response to the ambiance temperature change due to the lower thermal conductivity of polymers, e.g., ZnO/PET and ZnO/Trimetal/PET. Although the PET layer itself reduces the quality factor and efficiency of the acoustic operation of the devices as discussed, introducing a Trimetal layer between the ZnO and PET layers enhances the acoustic efficiency. These devices with various wavelengths were exposed to UV exposure to explore their responses. We observed that devices with larger wavelengths have a stronger response to the exposure of UV. We also tested all types of fabricated devices for their microfluidic pumping capability. Among these substrates, the devices fabricated on ZnO/Trimetal had the best performance for actuation. On the other hand, the devices fabricated on ZnO/Trimetal/PET led to an actuation capability, which wasn't feasible for the devices on polymer substrates. Therefore, addition of thin metallic films between ZnO and polymer layers not only maintains various sensing capabilities of the sensor, but also leads to enhance the actuation capability of ZnO/polymer substrates. The proposed fabricated devices can be utilised as an integrated, mechanically conformal platform for wearable devices.

References

[1] L. R. Volpatti and A. K. Yetisen, 'Commercialization of microfluidic devices', *Trends in Biotechnology*, vol. 32, no. 7, pp. 347–350, Jul. 2014, DOI: https://doi.org/10.1016/j.tibtech.2014.04.010.

[2] S. K. Vashist, P. B. Luppa, L. Y. Yeo, A. Ozcan, and J. H. T. Luong, 'Emerging Technologies for Next-Generation Point-of-Care Testing', *Trends Biotechnol*, vol. 33, no. 11, Art. no. 11, Nov. 2015, DOI: 10.1016/j.tibtech.2015.09.001.

[3] X. Zhu, S. Yuan, Y. Ju, J. Yang, C. Zhao, and H. Liu, 'Water Splitting-Assisted Electrocatalytic Oxidation of Glucose with a Metal–Organic Framework for Wearable Nonenzymatic Perspiration Sensing', *Anal. Chem.*, vol. 91, no. 16, pp. 10764–10771, Aug. 2019, DOI: 10.1021/acs.analchem.9b02328.

[4] D. Maier *et al.*, 'Toward Continuous Monitoring of Breath Biochemistry: A Paper-Based Wearable Sensor for Real-Time Hydrogen Peroxide Measurement in Simulated Breath', *ACS Sens.*, vol. 4, no. 11, pp. 2945–2951, Nov. 2019, DOI: 10.1021/acssensors.9b01403.

[5] Y. Yang and W. Gao, 'Wearable and flexible electronics for continuous molecular monitoring', *Chemical Society Reviews*, vol. 48, no. 6, pp. 1465–1491, 2019.

[6] D. P. Cotton, I. M. Graz, and S. P. Lacour, 'A multifunctional capacitive sensor for stretchable electronic skins', *IEEE Sensors Journal*, vol. 9, no. 12, pp. 2008–2009, 2009.

[7] R. Dahiya, W. T. Navaraj, S. Khan, and E. O. Polat, 'Developing electronic skin with the sense of touch', *Information Display*, vol. 31, no. 4, pp. 6–10, 2015.

[8] R. Dahiya *et al.*, 'Large-area soft e-skin: The challenges beyond sensor designs', *Proceedings of the IEEE*, vol. 107, no. 10, pp. 2016–2033, 2019.

[9] W. Taube Navaraj *et al.*, 'Nanowire FET based neural element for robotic tactile sensing skin', *Frontiers in neuroscience*, vol. 11, p. 501, 2017.

[10] M. Xie *et al.*, 'Flexible multifunctional sensors for wearable and robotic applications', *Advanced Materials Technologies*, vol. 4, no. 3, p. 1800626, 2019.

[11] S. Zahertar, E. Laurin, L. E. Dodd, and H. Torun, 'Embroidered Rectangular Split-Ring Resonators for the Characterization of Dielectric Materials', *IEEE Sensors Journal*, vol. 20, no. 5, pp. 2434–2439, Mar. 2020, DOI: 10.1109/JSEN.2019.2953251.

[12] P. Lorwongtragool, E. Sowade, N. Watthanawisuth, R. R. Baumann, and T. Kerdcharoen, 'A novel wearable electronic nose for healthcare based on flexible printed chemical sensor array', *Sensors*, vol. 14, no. 10, pp. 19700–19712, 2014.

[13] Y. Kim *et al.*, 'Tailored Graphene Micropatterns by Wafer-Scale Direct Transfer for Flexible Chemical Sensor Platform', *Advanced Materials*, p. 2004827, 2020.

[14] S. Nakata, T. Arie, S. Akita, and K. Takei, 'Wearable, flexible, and multifunctional healthcare device with an ISFET chemical sensor for simultaneous sweat pH and skin temperature monitoring', *ACS sensors*, vol. 2, no. 3, pp. 443–448, 2017.

[15] L. Wang, J. A. Jackman, J. H. Park, E.-L. Tan, and N.-J. Cho, 'A flexible, ultra-sensitive chemical sensor with 3D biomimetic templating for diabetes-related acetone detection', *Journal of Materials Chemistry B*, vol. 5, no. 22, pp. 4019–4024, 2017.

[16] S. Nakata, M. Shiomi, Y. Fujita, T. Arie, S. Akita, and K. Takei, 'A wearable pH sensor with high sensitivity based on a flexible charge-coupled device', *Nature Electronics*, vol. 1, no. 11, pp. 596–603, 2018.

[17] J. F. Tressler, S. Alkoy, and R. E. Newnham, 'Piezoelectric sensors and sensor materials', *Journal of electroceramics*, vol. 2, no. 4, pp. 257–272, 1998.

[18] J. W. Grate, S. J. Martin, and R. M. White, 'Acoustic wave microsensors', *analytical Chemistry*, vol. 65, no. 21, pp. 940A-948A, 1993.

[19] F. R. R. Teles and L. P. Fonseca, 'Trends in DNA biosensors', *Talanta*, vol. 77, no. 2, pp. 606–623, 2008.

[20] S. Zahertar, Y. Wang, R. Tao, J. Xie, Y. Q. Fu, and H. Torun, 'A fully integrated biosensing platform combining acoustofluidics and electromagnetic metamaterials', *J. Phys. D: Appl. Phys.*, vol. 52, no. 48, p. 485004, Nov. 2019, DOI: 10.1088/1361-6463/ab3f7d.

[21] Y.-Q. Fu *et al.*, 'Engineering inclined orientations of piezoelectric films for integrated acoustofluidics and lab-on-a-chip operated in liquid environments', *Lab on a Chip*, 2020.

[22] R. Tao *et al.*, 'Integrating microfluidics and biosensing on a single flexible acoustic device using hybrid modes', *Lab on a Chip*, vol. 20, no. 5, pp. 1002–1011, 2020.

[23] A. Wixforth, 'Acoustically driven programmable microfluidics for biological and chemical applications', *JALA: Journal of the Association for Laboratory Automation*, vol. 11, no. 6, pp. 399–405, 2006.

[24] E. R. Gray *et al.*, 'Ultra-rapid, sensitive and specific digital diagnosis of HIV with a dual-channel SAW biosensor in a pilot clinical study', *NPJ digital medicine*, vol. 1, no. 1, pp. 1–8, 2018.

[25] L. Lamanna, F. Rizzi, V. R. Bhethanabotla, and M. De Vittorio, 'Conformable surface acoustic wave biosensor for E-coli fabricated on PEN plastic film', *Biosensors and Bioelectronics*, vol. 163, p. 112164, 2020.

[26] R. Tao *et al.*, 'Bimorph material/structure designs for high sensitivity flexible surface acoustic wave temperature sensors', *Scientific reports*, vol. 8, no. 1, pp. 1–9, 2018.

[27] X. Tao *et al.*, 'Three-dimensional tetrapodal ZnO microstructured network based flexible surface acoustic wave device for ultraviolet and respiration monitoring applications', *ACS Applied Nano Materials*, vol. 3, no. 2, pp. 1468–1478, 2020.

[28] Y. J. Guo *et al.*, 'Ultraviolet sensing based on nanostructured ZnO/Si surface acoustic wave devices', *Smart Materials and Structures*, vol. 24, no. 12, p. 125015, 2015.

[29] Y. Liu *et al.*, 'Flexible and bendable acoustofluidics based on ZnO film coated aluminium foil', *Sensors and Actuators B: Chemical*, vol. 221, pp. 230–235, 2015.

[30] R. Tao *et al.*, 'Hierarchical nanotexturing enables acoustofluidics on slippery yet sticky, flexible surfaces', *Nano letters*, vol. 20, no. 5, pp. 3263–3270, 2020.

[31] C. Jagadish and S. J. Pearton, Zinc oxide bulk, thin films and nanostructures: processing, properties, and applications. *Elsevier*, 2011.

[32] L. Lamanna *et al.*, 'Flexible and Transparent Aluminum-Nitride-Based Surface-Acoustic-Wave Device on Polymeric Polyethylene Naphthalate', *Advanced Electronic Materials*, vol. 5, no. 6, p. 1900095, 2019.

[33] M. Smith and S. Kar-Narayan, 'Piezoelectric Polymers: theory, challenges and opportunities', *International Materials Reviews*, pp. 1–24, 2021.

[34] A. Kumar, G. Thachil, and S. Dutta, 'Ultra high frequency acoustic wave propagation in fully polymer based surface acoustic wave device', *Sensors and Actuators A: Physical*, vol. 292, pp. 52–59, 2019.

[35] U. V. Aniekwe and T. A. Utigard, 'High-temperature oxidation of nickel-plated copper vs pure copper', *Canadian metallurgical quarterly*, vol. 38, no. 4, pp. 277–281, 1999.

[36] 'Types of Nickel Plating and Its Benefits | Dorsetware', Dorsetware Limited, Apr. 02, 2016. https://www.dorsetware.com/types-nickel-plating/ (accessed Jan. 06, 2021).

[37] 'Nickel Plated Copper'. https://www.elektrisola.com/conductor-materials/plated-wires/nickel-plated-copper.html (accessed Jan. 06, 2021).

[38] S. Zahertar, R. Tao, H. Torun, P. Canyelles-Pericas, and Y.-Q. Fu, 'Integrated Sensing and Actuation Capabilities of Flexible Surface Acoustic Wave Devices with Metallic and Polymer Layers', in *2021 IEEE International Conference on Flexible and Printable Sensors and Systems (FLEPS)*, 2021, pp. 1–4.

[39] 'datasheets_S1800.pdf'. Accessed: May 25, 2021. [Online]. Available: https://amolf.nl/wp-content/uploads/2016/09/datasheets_S1800.pdf

[40] J. W. Grate, S. W. Wenzel, and R. M. White, 'Flexural plate wave devices for chemical analysis', *Analytical Chemistry*, vol. 63, no. 15, pp. 1552–1561, 1991.

[41] T. Laurent, F. O. Bastien, J.-C. Pommier, A. Cachard, D. Remiens, and E. Cattan, 'Lamb wave and plate mode in ZnO/silicon and AlN/silicon membrane: Application to sensors able to operate in contact with liquid', *Sensors and Actuators A: Physical*, vol. 87, no. 1–2, pp. 26–37, 2000.

[42] N. T. Nguyen and R. M. White, 'Design and optimization of an ultrasonic flexural plate wave micropump using numerical simulation', *Sensors and Actuators A: Physical*, vol. 77, no. 3, pp. 229–236, 1999.

[43] R. M. Moroney, R. M. White, and R. T. Howe, 'Microtransport induced by ultrasonic Lamb waves', *Applied physics letters*, vol. 59, no. 7, pp. 774–776, 1991.

[44] S. J. Martin, G. C. Frye, and S. D. Senturia, 'Dynamics and response of polymer-coated surface acoustic wave devices: effect of viscoelastic properties and film resonance', *Analytical Chemistry*, vol. 66, no. 14, pp. 2201–2219, 1994.

[45] Y. Q. Fu *et al.*, 'Advances in piezoelectric thin films for acoustic biosensors, acoustofluidics and lab-on-chip applications', *Progress in Materials Science*, vol. 89, pp. 31–91, 2017.

[46] Y. J. Guo *et al.*, 'Ultraviolet sensing based on nanostructured ZnO/Si surface acoustic wave devices', *Smart Materials and Structures*, vol. 24, no. 12, p. 125015, 2015.

[47] R. Tao *et al.*, 'Flexible and Integrated Sensing Platform of Acoustic Waves and Metamaterials based on Polyimide-Coated Woven Carbon Fibers', *ACS sensors*, vol. 5, no. 8, pp. 2563–2569, 2020.

Shahrzad Zahertar Shahrzad Zahertar is a research fellow at the Optoelectronics Research Centre (ORC) at the University of Southampton. Prior to that, she was a research fellow at the Department of Mathematics, Physics and Electrical Engineering at Northumbria University, UK. She received her PhD degree in electrical engineering from Northumbria University, UK, MSc degree in electrical and electronics engineering from Bogazici University, Turkey and BSc degree in electrical engineering-bioelectric from University of Tehran, Iran. Her current research interests include flat optical fibres for sensing applications, metamaterials for biosensing applications, Surface Acoustic Wave (SAW) actuators, and Lab on Chip devices.

Ran Tao received the B.Eng. degree from Tsinghua University, Beijing, China in 2011, the M.Eng. degree from Ecole Centrale de Lyon, Université Claude Bernard Lyon 1 and Institut National des Sciences Appliquées in Lyon, France in 2013, and the Ph.D. degree from University of Grenoble Alpes, CNRS, Grenoble INP, Grenoble, France in 2017. She worked as a research fellow in University of Northumbria at Newcastle, UK from 2017 to 2020. Now she works as an assistant professor in College of physics and optoelectronic engineering, Shenzhen University, China. Her research interests include flexible and bendable SAW sensors and acoustofluidics devices.

Hongzhe Wang received the B.S. degree in information engineering from Chengdu University of Technology (CDUT), Chengdu, China, in 2016. He is currently pursuing the Ph.D. degree in microelectronics at University of Electronic Science and Technology of China (UESTC), Chengdu, China. His research interests include surface acoustic wave devices, memristor, and their applications in artificial intelligence.

Hamdi Torun is an associate professor at Northumbria University. Previously, he was an associate professor at Bogazici University, Turkey. He is a cofounder of GlakoLens, a biomedical spinoff company. He received Technology Award from Elginkan Foundation, Turkey in 2016, Young Scientist Award from The Science Academy, Turkey in 2016, Innovator Under 35 Award from MIT Tech Review in 2014, and Marie Curie Fellowship (MC-IRG Grant) in 2011. His expertise is in development of integrated micro/nanosystems especially for sensing applications.

Pep Canyelles-Pericas (Member, IEEE) received the double degree in B.Eng. electrical and electronic engineering from the Technical University of Catalonia, Barcelona, Spain, and the University of Northumbria, Newcastle upon Tyne, U.K., in 2006, the M.Sc. degree in engineering management from the University of Sunderland, Sunderland, U.K., in 2008, and the Ph.D. degree in control systems (he studied nonlinear state observers) from the University of Northumbria, in 2016. Between 2009 and 2012, he worked as Optoelectronics Research Engineer with the University of the Balearic Islands, Palma, Spain. After Ph.D. graduation, he engaged with Innovate U.K. projects in the Knowledge Transfer Partnership (KTP) and the Innovation to Commercialization of University Research (ICURe) schemes. Since 2019, he has been a Researcher with the MESA+ Institute of Nanotechnology, University of Twente, Enschede, The Netherlands. His research interests are acoustofluidics, optical sensing, instrumentation, and control.

Yang Liu received the B.Sc. degree in microelectronics from Jilin University, China, in 1998, and the Ph.D. degree from Nanyang Technological University, Singapore, in 2005. From 2005 to 2006, he was a Research Fellow with Nanyang Technological University. In 2006, he was awarded the prestigious Singapore Millennium Foundation Fellowship. In 2008, he joined the School of Microelectronics, University of Electronic Science and Technology, China, as a Full Professor. He has authored or coauthored over 130 peer-reviewed journal papers and more than 100 conference papers. He holds one U.S. patent and more than 30 China patents also. His current research interests include memristor neural network systems, neuromorphic computing ICs, and AI-RFICs.

Jethro Vernon received his MEng (Hons) in Electrical and Electronic Engineering from the University of Northumbria, U.K in 2018. Since 2018, he is a PhD candidate in the same university. He is currently working with piezo electric thin film surface acoustic waves for biomedical applications. His experience and expertise is in the integration of electronics, sensors, and software.

Wai Pang Ng (S'99-M'01-SM'08) received his BEng (Hons) in Communications and Electronic Engineering, from the University of Northumbria, U.K. and his Ph.D. in Electronic Engineering from University of Wales, Swansea. He is currently the Deputy Head of Department and Associate Professor of Optical Communications in the Department of Maths, Physics and Electrical Engineering, Northumbria University, U.K. He has worked as Senior Networking Software Engineer at Intel Corporation. His research interests include radio-over-fibre, cognitive radio, high speed optical communications, adaptive digital signal processing and distributed fibre sensing.

Richard Binns is the Head of Department of Mathematics Physics and Electrical Engineering and Associate Professor at Northumbria University. He is currently responsible for a department of 60 staff a member of the faculty executive routinely headed up professional body accreditations and establishing collaborative links to institutions in Malaysia, Singapore and China. Dr Richard Binns graduated from Huddersfield University with a degree in Electronic and Information Engineering in 1993 and also a PhD in Analogue Test strategies in 1997. He moved to Northumbria University in 2001 on an EPSRC post-doctoral contract looking into Analogue Synthesis tool development in collaboration with Ericson Components and Cadence Design Systems. Current research works is varied from design of electronics for visible light communications, energy management in electric vehicles, research into radiation detection mechanisms for personal dosimetry and power control systems development.

Qiang Wu Qiang Wu received the B.S. and Ph.D. degrees from Beijing Normal University and Beijing University of Posts and Telecommunications, Beijing, China, in 1996 and 2004, respectively. From 2004 to 2006, he worked as a Senior Research Associate in City University of Hong Kong. From 2006 to 2008, he took up a research associate post in Heriot-Watt University, Edinburgh, U.K. From 2008 to 2014, he worked as a Stokes Lecturer at Photonics Research Centre, Dublin Institute of Technology, Ireland. He is an Associate Professor / Reader with Faculty of Engineering and Environment, Northumbria University, Newcastle Upon Tyne, United Kingdom. His research interests include optical fiber interferometers for novel fiber optical couplers and sensors, nanofiber, microsphere sensors for bio-chemical sensing, the design and fabrication of fiber Bragg grating devices and their applications for sensing, nonlinear fibre optics, surface plasmon resonant and surface acoustic wave sensors. He has over 200 publications in the area of photonics and holds 3 invention patents. He is an Editorial Board Member of Scientific Reports, an Associate Editor for IEEE Sensors Journal and an Academic Editor for Journal of Sensors.

Jingting Luo received the Ph.D. degree from Tsinghua University, Beijing, China, in 2012. Since 2012, he has been working as a researcher in Shenzhen University. He worked as an Academic Visitor in 2016 at the Faculty of Engineering and Environment, University of Northumbria at Newcastle,U.K. He is currently an Professor with in the College of Physics and optoelectronic engineering, Shenzhen University, Shenzhen, China.

Richard (YongQing) Fu is a professor in the Faculty of Engineering and Environment, University of Northumbria at Newcastle, UK. He obtained his PhD degree in 1999 from Nanyang Technological University, Singapore, and then worked as a Research Associate in University of Cambridge. He was a lecturer in Heriot-Watt University, Edinburgh, UK, and then a Reader in Thin Film Centre in University of West of Scotland, Glasgow, UK, before moving to Newcastle, UK in 2015. He has extensive experience in smart thin films/materials, biomedical microdevices, energy materials, lab-on-chip, micromechanics, MEMS, nanotechnology, sensors and microfluidics. He published over 400 science citation index (SCI) journal papers and his current SCI H-index is 58.